AN ELECTROSTATIC ANALOG FOR GENERATING CASCADE GRIDS

John J. Adamczyk
NASA Lewis Research Center

ABSTRACT

Accurate and efficient numerical simulation of flows through turbomachinery blade rows depends on the topology of the computational grids. These grids must reflect the periodic nature of turbomachinery blade row geometries and conform to the blade shapes. Three types of grids can be generated that meet these minimal requirements: (1) through-flow grids, (2) O-type grids, and (3) C-type grids. This paper presents a procedure which can be used to generate all three types of grids. The resulting grids are orthogonal and can be stretched to capture the essential physics of the flow. In addition, a discussion is also presented detailing the extension of the generation procedure to three-dimensional geometries.

BLADE GEOMETRY AND COORDINATES

The development of the grid generation procedure begins by considering the electrostatic potential field generated by an infinite linear array of point charges in a two-dimensional space. The density of the charges is assumed to alternate between plus and minus 1. The mathematical expression for the complex electrostatic field is given by equation (1), where $K(z - z_o)$ is the complex potential and $i = \sqrt{-1}$. For a Cartesian space $z = x + iy$, z_o is the location of the zeroth charge and s is the physical distance between charges. For a blade row whose geometry is given on a blade-to-blade surface of revolution, $z = m + i\theta$, where m is the meridional distance and θ is the angular position; s then represents the angular distance between charges.

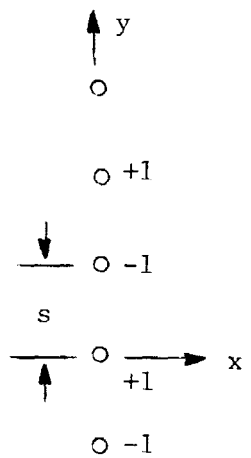

Array of point charges

$$K(z - z_o) = \sum_{n=-\infty}^{\infty} (-1)^n \ln(z - z_o - ins) \qquad (1)$$

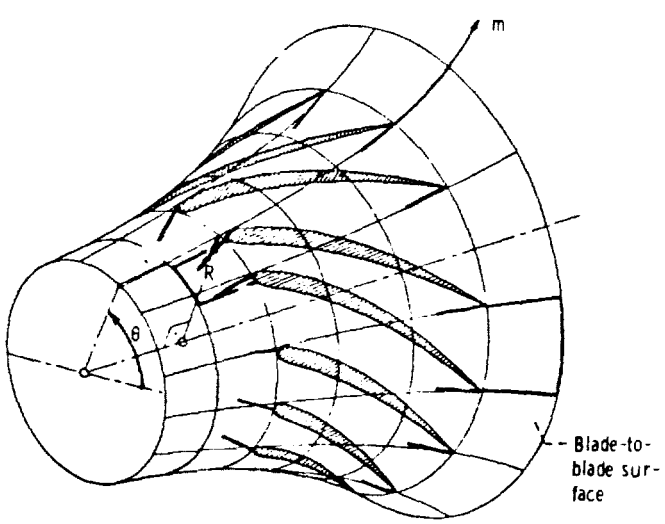

Blade-to-blade surface of revolution, showing m - θ coordinates.

DEVELOPMENT OF EQUATION FOR POTENTIAL FIELD SURROUNDING THE BLADE

The field equation for the array of point charges is expressed in closed form in equation (2). Note that this expression is periodic in either the y- or θ-direction with period 2s. The potential field generated by distributing the fundamental solution (eq. (2)) over the surface of a blade is given by equation (3), where $\gamma(z_o)$ is the source density distribution on the blade surface. It is required that the real part of ω (that is, ξ) be equal to 1 on the blade surface (eq. (4)). At large distances upstream or downstream of the cascade, $\xi(z)$ is assumed to approach zero. This additional requirement is expressed by equation (5). Equation (3) evaluated on the blade surface forms a singular integral equation, equation (6), for the source density. Once γ is known, the potential field surrounding the blade can be computed by direct integration of equation (3).

$$K(z - z_o) = \sum_{n=-\infty}^{\infty} (-1)^n \ln(z - z_o - ins) = \ln \tanh \frac{(z - z_o)\pi}{2s} \tag{2}$$

$$\omega(z) = \int_L \gamma(z_o) K(z - z_o) dz_o \tag{3}$$

$$\text{Real } \omega(z) = \xi(z) \equiv 1 \qquad (z \in L) \tag{4}$$

$$\text{Im} \int_L \gamma(z_o) dz_o = 1 \tag{5}$$

$$1 = \text{Real} \left[\int_L \gamma(z_o) K(z - z_o) dz_o \right] \qquad (z \in L) \tag{6}$$

DEVELOPMENT OF EQUATIONS FOR SOURCE DENSITY DISTRIBUTION

The singular integral equations for γ can be solved by paneling methods similar to those used in solving potential flow problems in fluid mechanics. To employ these procedures, one first factors out of the integral equation its singular behavior. (For eq. (6) the factored form is expressed by eq. (7).) Next the blade surface L is divided into a series of segments. Over each of these segments $\gamma(z_o)$ and $\ln\left[\frac{2s}{(z - z_o)\pi} \tanh (z - z_o) \frac{\pi}{2s}\right]$ are approximated by polynomials in z_o. For the cases examined to date it was found that these terms could be approximated by a constant equal to their value at the midpoint of each segment. (This approximation assumes the length of the segment could be made smaller than the scale of the local geometric blade features.) Thus the singular part of equation (7) integrated over a segment is approximated by equation (8), while the regular part is approximated by equation (9). The auxiliary condition (eq. (6)) is approximated over a segment by equation (10). Upon introducing these approximations into equation (7) and restricting the value of z_o to the midpoint of each segment, a system of linear algebraic equations is obtained from which $\gamma(z_o)$ can be determined.

$$1 = \text{Real}\left[\int_L \gamma(z_o) \ln \frac{(z - z_o)\pi}{2s} \, dz_o + \int_L \gamma(z_o) \ln \frac{2s}{(z - z_o)\pi} \tanh \frac{(z - z_o)\pi}{2s} \, dz_o\right] \tag{7}$$

$$\int_a^b \gamma(z_o) \ln \frac{(z - z_o)\pi}{2s} \, dz_o \approx \gamma(z_o)\Big[(z - b) \ln (z - b) - (z - a) \ln (z - a) + b - a\Big]\Big|_{z_o=\frac{b+a}{2}} \tag{8}$$

$$\int_a^b \gamma(z_o) \ln \frac{2s}{(z - z_o)\pi} \tanh \frac{(z - z_o)\pi}{2s} \, dz_o \approx \gamma(z_o)\left[(b - a) \ln \frac{2s}{(z - z_o)\pi} \tanh \frac{(z - z_o)\pi}{2s}\right]\Bigg|_{z_o=\frac{b+a}{2}} \tag{9}$$

$$\text{Im} \int_a^b \gamma(z_o) dz_o \approx \text{Im}\left[\gamma(z_o)(b - a)\right]\Big|_{z_o=\frac{b+a}{2}} \tag{10}$$

BOUNDARIES OF COMPLEX ELECTROSTATIC FIELD SURROUNDING THE BLADE

With γ known, the complex electrostatic field surrounding the blade sections can be found. The real part ξ and the imaginary part η of the field form a periodic orthogonal body-fitted coordinate system. The contours ξ = Constant enclose the blade, while the curves η = Constant project from the blade (i.e., $\xi = 1$) to the periodic boundary ($\xi = 0$). The curves extending to upstream and downstream infinity are denoted $\eta = 0$, $\eta = \pm L$, respectively. The locations of these bounding coordinate curves are found using a Newton-Raphson scheme with equation (3) to numerically generate the inverse mapping function. This procedure, however, because of its slow computational speed, was not used to construct the interior grid contours.

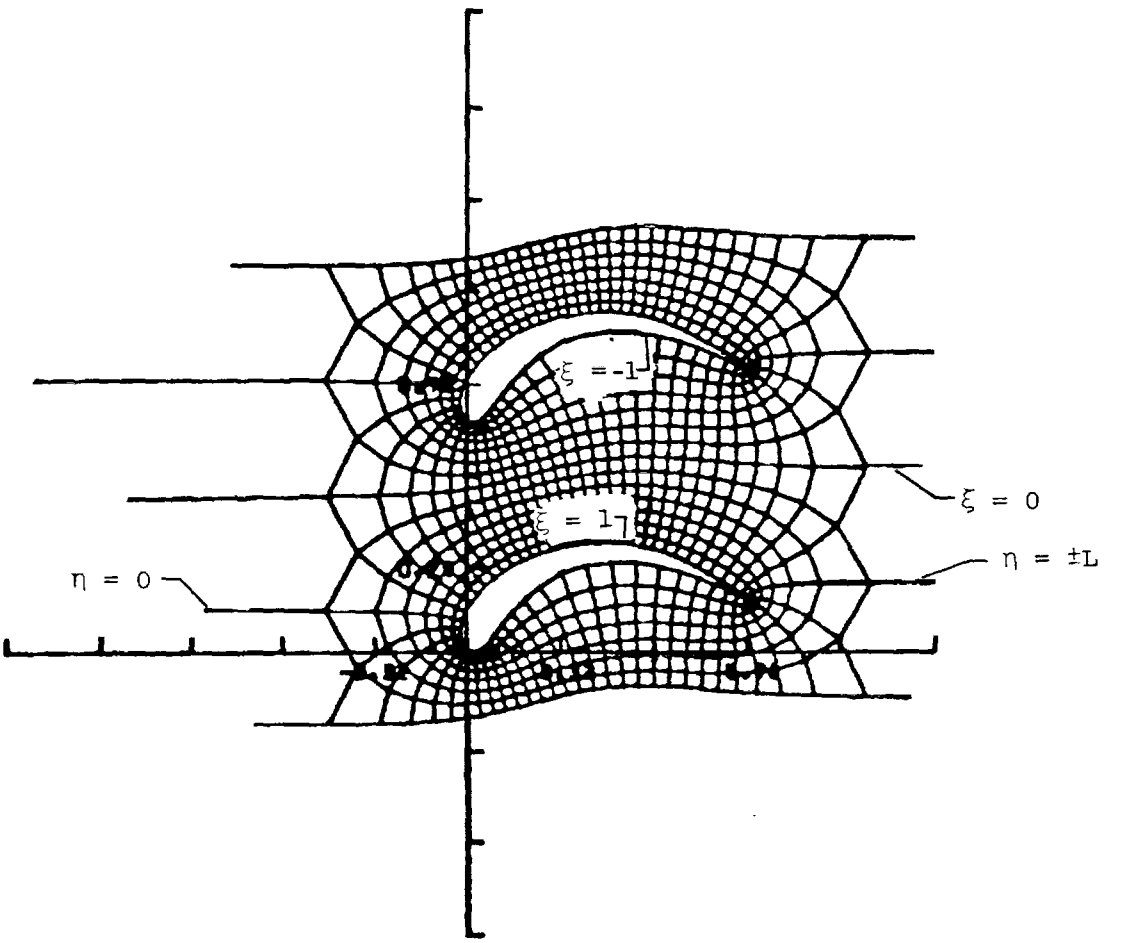

INTERIOR GRID

The interior grid points are constructed from the solution of the inverse electrostatic problem in which (x,y) or (m,θ) are specified as functions of ξ or η on the boundaries. The field equation for this is Laplace's equation in terms of (ξ,η) (eq. (11)). The solution of equation (11) which satisfies boundary conditions consistent with the coordinates of the bounding curvilinear curves yields the interior grid geometry. This solution can be obtained by either numerical or analytical procedures.

$$\frac{\partial^2(x,m)}{\partial\xi^2} + \frac{\partial^2(x,m)}{\partial\eta^2} = 0$$

$$\frac{\partial^2(y,m)}{\partial\xi^2} + \frac{\partial^2(y,\theta)}{\partial\eta^2} = 0 \qquad (11)$$

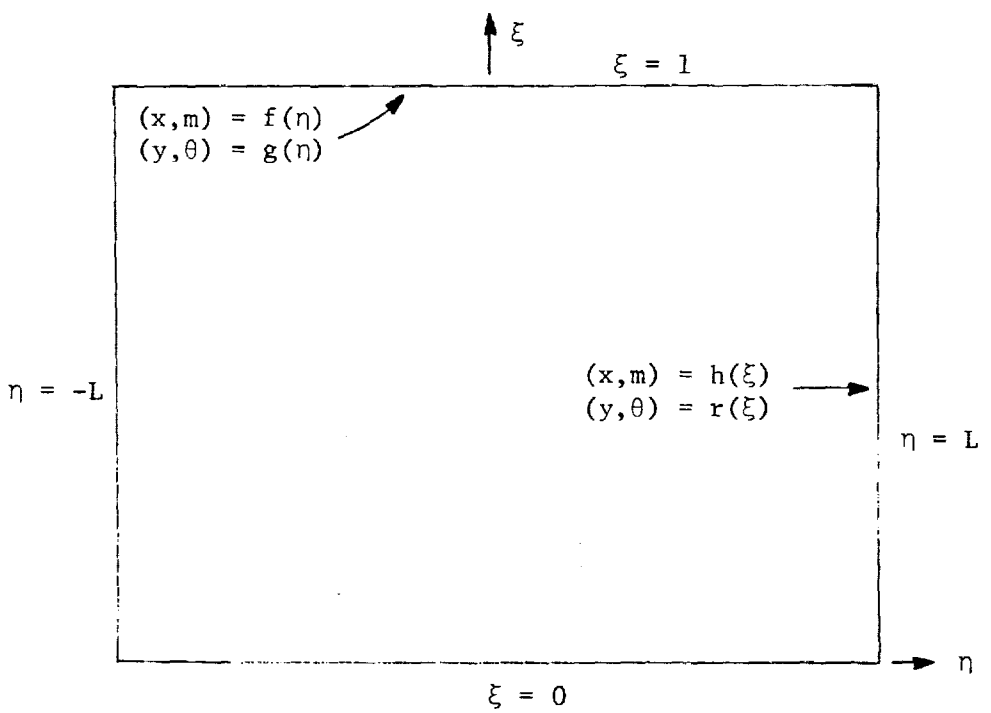

GRID CLUSTERING

Grid clustering to capture the physics of the flow field can be introduced prior to or after the solution of the inverse problem is obtained. To insure orthogonality, the stretching functions used for clustering must be one-dimensional (i.e., eqs. (12)). The ξ transformation can be quite arbitrary. For potential flow computations, a linear transformation is generally used. For viscous flows, one attempts to cluster grid points near the blade surface. An example of a transformation which can be used for this purpose is given by equation (13). The parameters m_o, m_1 control the degree of stretching in the transformation. The clustering of grid points in the η-direction requires special consideration to insure that grid point periodicity is maintained. A grid point located on the periodic boundary at $\eta = \eta_o$ has an image at $\eta = -\eta_o$. In order to maintain this property, the transformation in η must be an odd function of $\tilde{\eta}$ over the interval $-L$ to L. A simple transformation which exhibits this behavior is a polynomial in odd powers of $\tilde{\eta}$, an example being given by equation (14). The parameters m_o and m_1 in this transformation are again used to control the degree of clustering.

$$\left.\begin{aligned} \xi &= \xi(\tilde{\xi}) \qquad (0 \le \tilde{\xi} \le 1) \\ \eta &= \eta(\tilde{\eta}) \qquad (-L \le \tilde{\eta} \le L) \end{aligned}\right\} \tag{12}$$

$$\xi = m_o\tilde{\xi} + (3 - m_1 - 2m_o)\tilde{\xi}^2 + (m_1 + m_o - 2)\tilde{\xi}^3 \tag{13}$$

$$\eta = m_o\tilde{\eta} + \frac{1}{2L^2}(5 + 4m_o - m_1)\tilde{\eta}^3 - \frac{1}{2L^4}(3 - 2m_o - m_1)\tilde{\eta}^3 \tag{14}$$

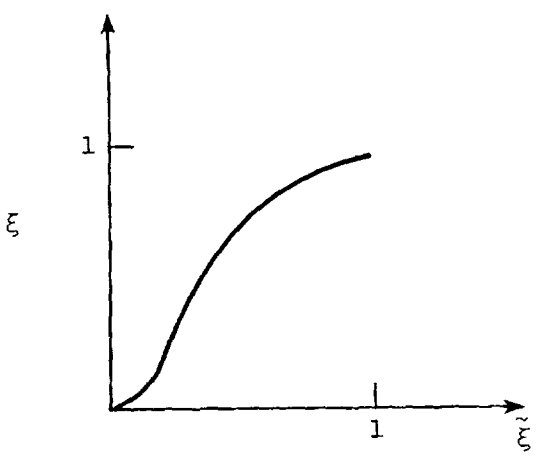

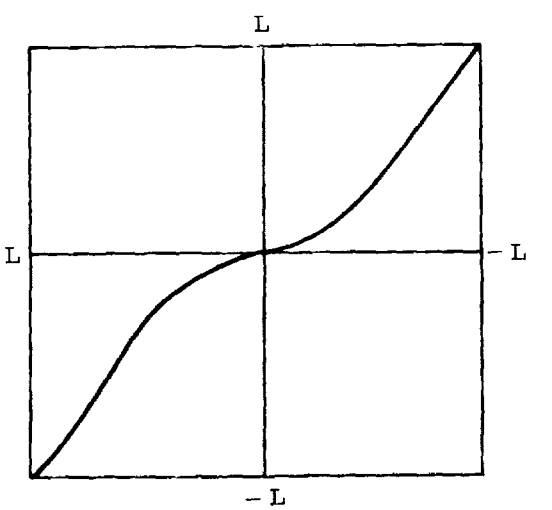

GENERATION OF C-TYPE AND THROUGH-FLOW GRIDS

Thus far the application of the grid generation procedure has been restricted to orthogonal O-type grids. To generate through-flow and C-type grids by the current procedure, the blade contours must be modified by appending slits of zero thickness to their surfaces. For C-type grids, one slit is used. Its origin is generally taken to be the trailing edge of the blade. For through-flow grids, two slits are appended, their origins being the leading and trailing edges of the blade. The shape of these appendages can be quite general. The generation of the grids associated with these modified blade profiles proceeds as in the O-grid procedure outlined above. The generated grids are orthogonal and periodic. In the case of blunt blades, however, they exhibit a singular behavior at the slit attachment point.

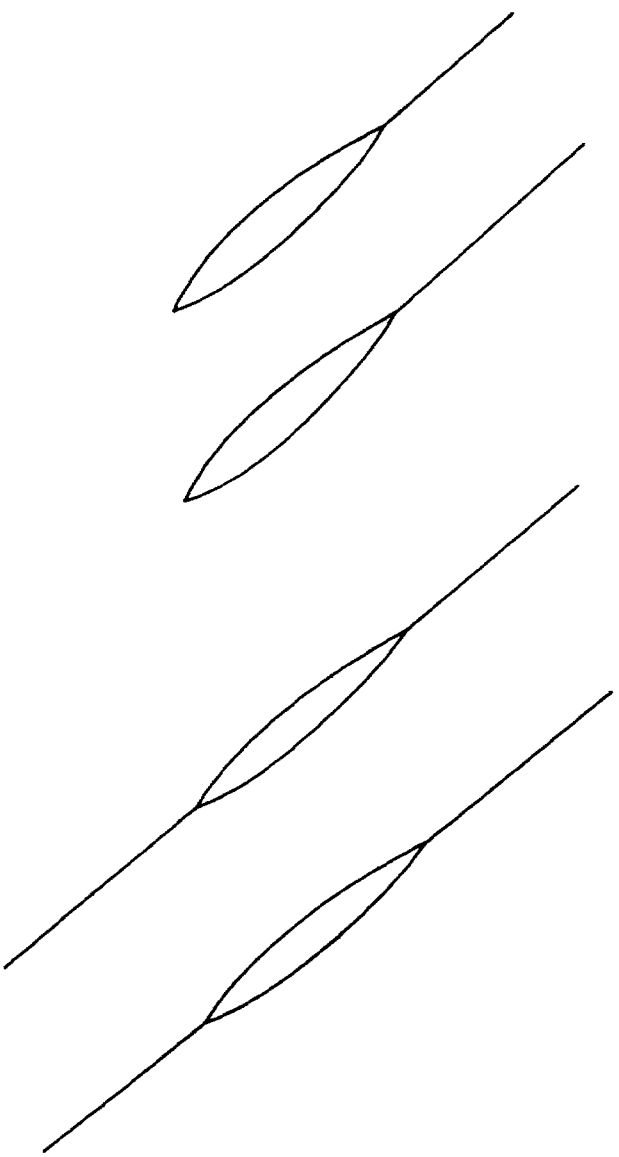

For cascades of nonzero stagger, the C-type or through-flow grids generated by the current procedure are discontinuous across the slit. This undesirable property can be corrected by a simple construction. First the two grid lines connecting the upper periodic boundary and the trailing edge and the lower periodic boundary and the trailing edge are found. Next the location and value of η corresponding to the periodic image of A on the lower boundary (i.e., A') and B' on the upper boundary (i.e., B) are determined. The spacing of grid points along the slit between EF is specified, which in turn determines the distribution of η along both sides of the slit. This in turn determines the distribution of η along the periodic boundaries AB and B'C'. The grid points along A'B' are required to be periodic images of the points along AB. This determines the distribution of η along A'B' and the grid geometry up to EB'. The construction of the grid downstream of $\bar{BrC}'$ proceeds in the same manner as outlined above, with the grid spacing along B'C' defining the clustering pattern. The resulting grids will remain orthogonal and periodic under this construction procedure.

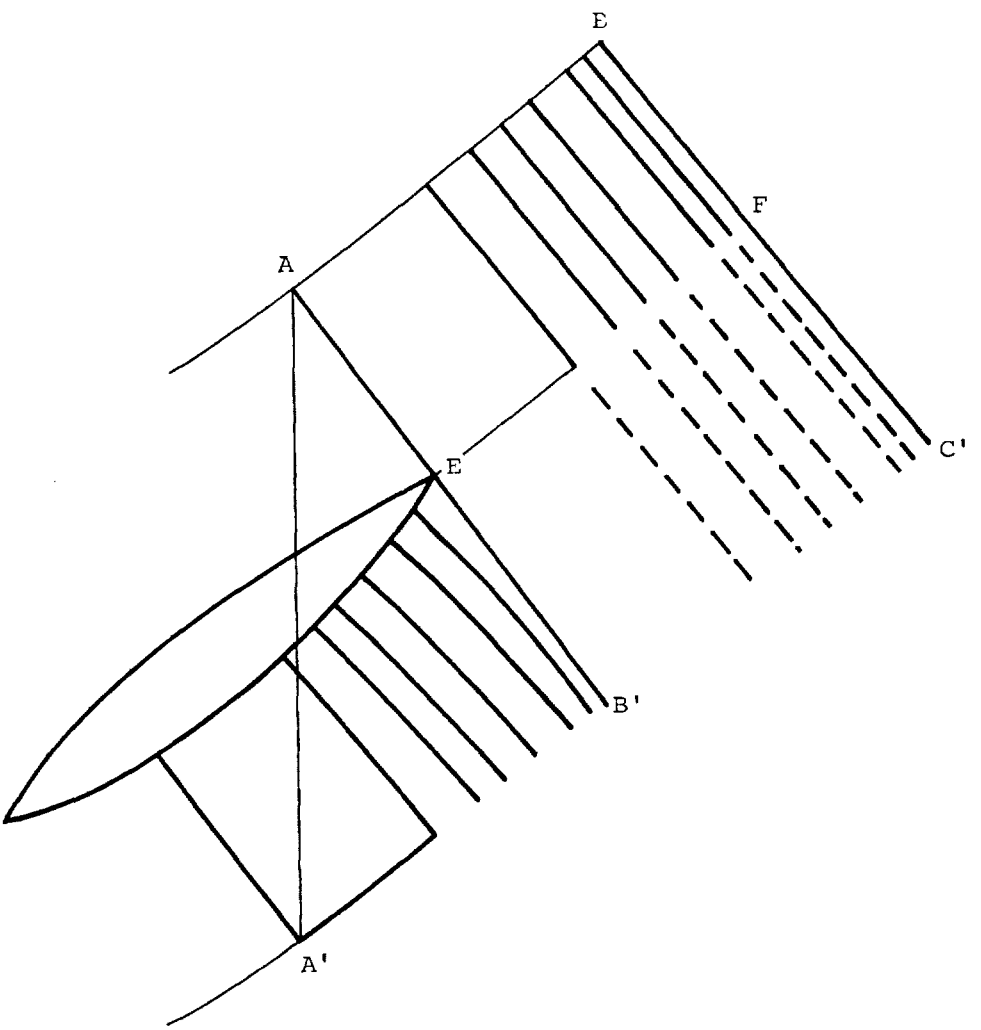

DEVELOPMENT OF THREE-DIMENSIONAL GRIDS

Three-dimensional grids can also be developed by the current procedure. The geometry of a typical blade assembly as viewed in the meridional plane is shown in the accompanying figure. Let the surfaces of revolution describing the hub and shroud be denoted by $r = f_H(x)$, $r = f_S(x)$. A surface of revolution bounded by these limits is given by equation (15). Similarly, let m denote the percentage of distance measured from the leading edge of the blade along the surfaces of revolution (eq. (16)). On a surface of revolution the blade section geometry is given in terms of m and θ, where θ is the angular location around the wheel. On the blade surface of revolution m and θ can be expressed in terms of the coordinates ξ,η of the current orthogonal system. The resulting coordinate system (ζ,ξ,η) will be orthogonal on a ζ-plane and conform to the blade hub and shroud surface.

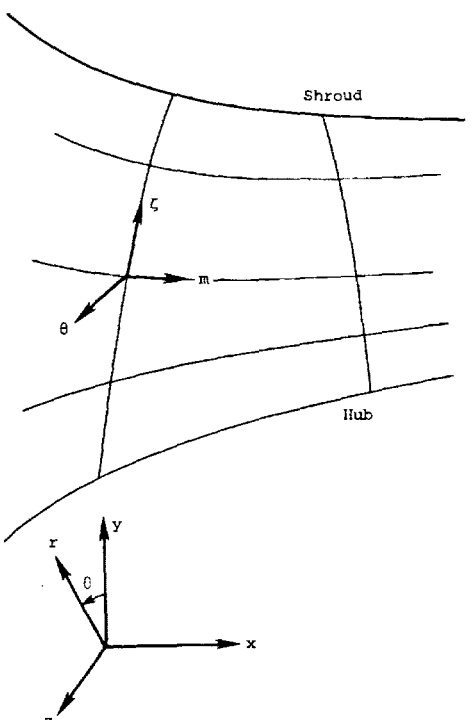

$$\zeta = \frac{r - f_H(x)}{f_S(x) - f_H(x)} \qquad (f_H \le r \le f_S) \tag{15}$$

$$m = \frac{\int_0^{m_\zeta} ds}{\int_0^{L_\zeta} ds} \tag{16}$$

EXAMPLE O-TYPE GRID FOR TURBINE STATOR BLADE

An example of an O-type grid generated by the current procedure is shown on the accompanying figure. The blade is a turbine stator with approximately 90° of turning. No stretching was introduced in developing the grid. In regions of high surface curvature there is a high concentration of grid points, thus permitting accurate resolution of the local flow physics. Far removed from the blade, the concentration of grid points becomes sparse. This results in an economical distribution of grid points in regions of uniform flow. The grid as shown was generated to solve a potential flow problem. For viscous flow, a stretching of the ξ contours would have to be introduced to capture the boundary-layer region. In addition, the η lines would have to be clustered in the trailing-edge region to resolve the viscous wake.

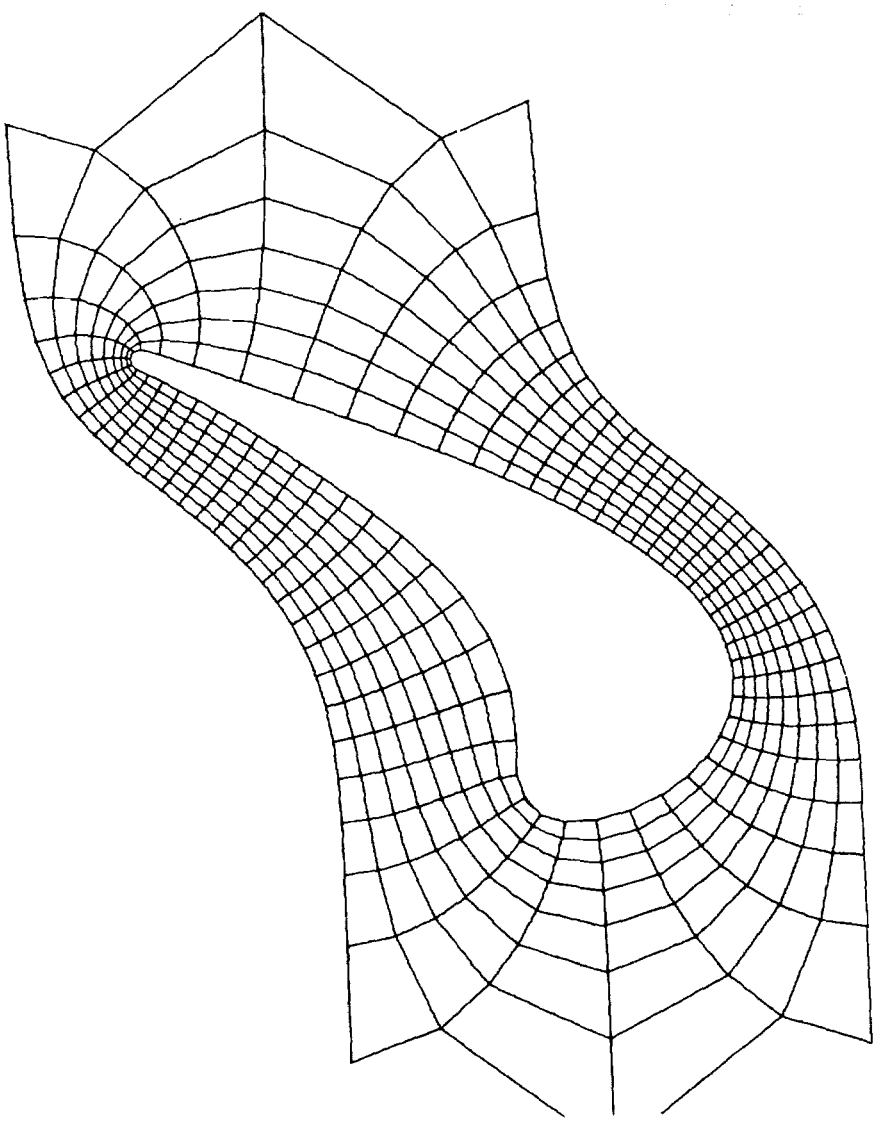

EXAMPLE THROUGH-FLOW GRID FOR A TURBINE ROTOR BLADE

The next example is a through-flow grid for a high-reaction turbine rotor. This grid, as described earlier in the paper, was generated by appending two slits to the blade surfaces. The grid geometry is rectangular and periodic upstream and downstream of the cascade. Across the wake the grid geometry is seen to be discontinuous. The use of such a grid would require special care in transferring flow variables across the slit.

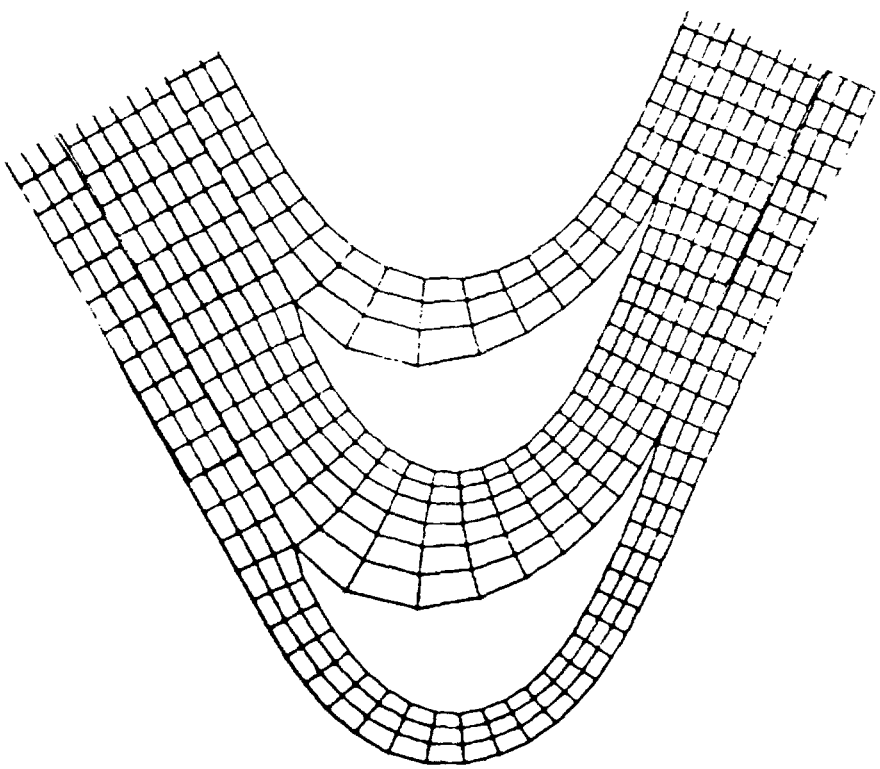

EXAMPLE C-TYPE GRID FOR A TURBINE ROTOR BLADE

The accompanying figure shows a C-type grid for the preceding turbine blade. Upstream of the blade the grid geometry is similar to an O-type grid, while downstream it resembles a through-flow grid. For this grid the construction procedure outlined earlier was used to insure continuous grid geometry across the slit. For potential flow analysis the grid as shown is quite suitable. For viscous analysis a clustering of the grid lines near the blade surface and trailing-edge region would have to be introduced to accurately resolve the flow physics.

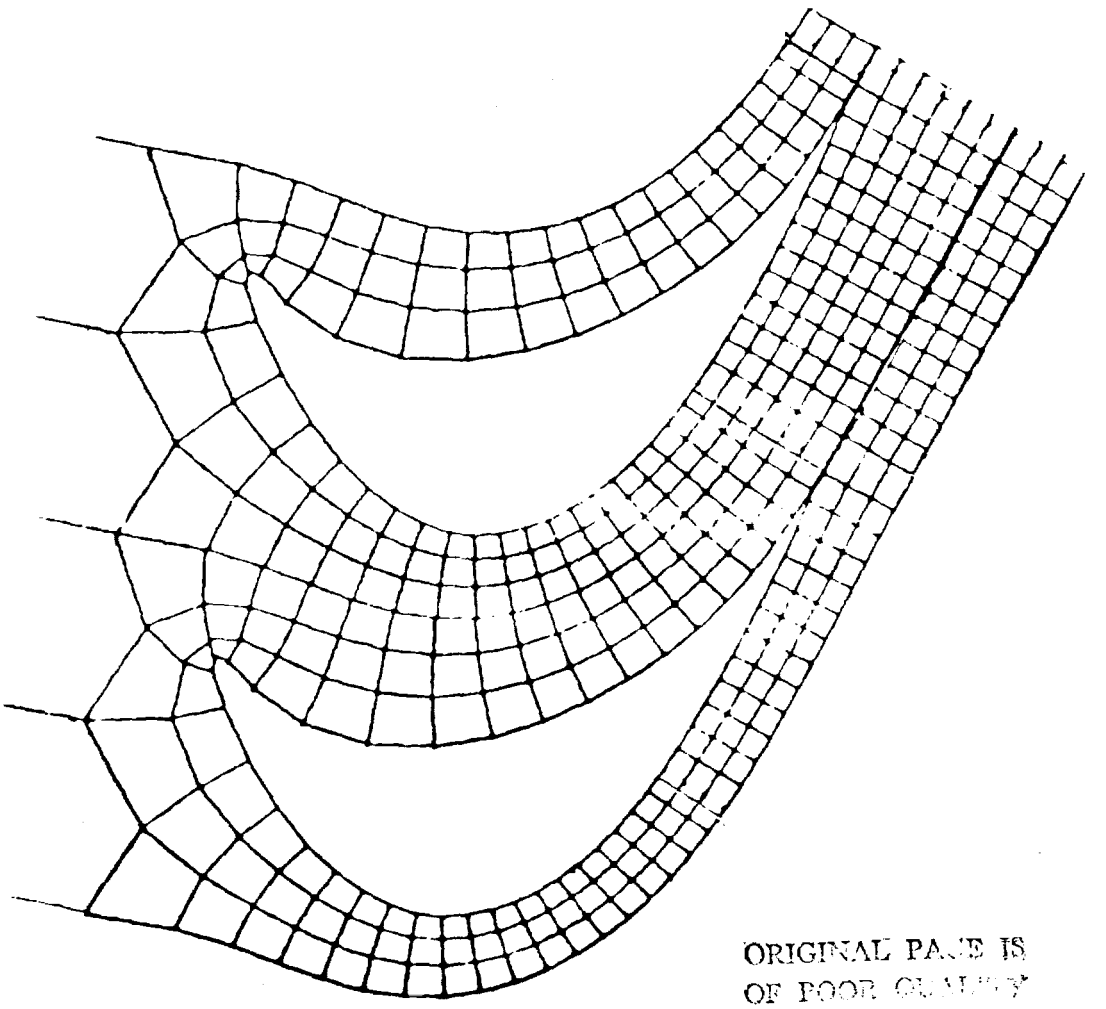

EXAMPLE C-TYPE GRID FOR CASCADE OF NACA 0012 AIRFOILS

The final example is a C-type grid for a cascade of NACA 0012 airfoils. This grid was generated by When-Huei Jou of Flow Research. The grid generation procedure as modified by him produces grids which are nearly orthogonal. The slight nonorthogonality is due to stretching functions used to maintain continuous grid geometry across the slit and cascade periodicity. This grid was generated to solve a two-dimensional potential flow problem. It can also be used to solve a three-dimensional potential flow problem, provided the inviscid wake is convected downstream along the slit. For viscous flow calculation a clustering of grid points near the body and wake region would have to be introduced.

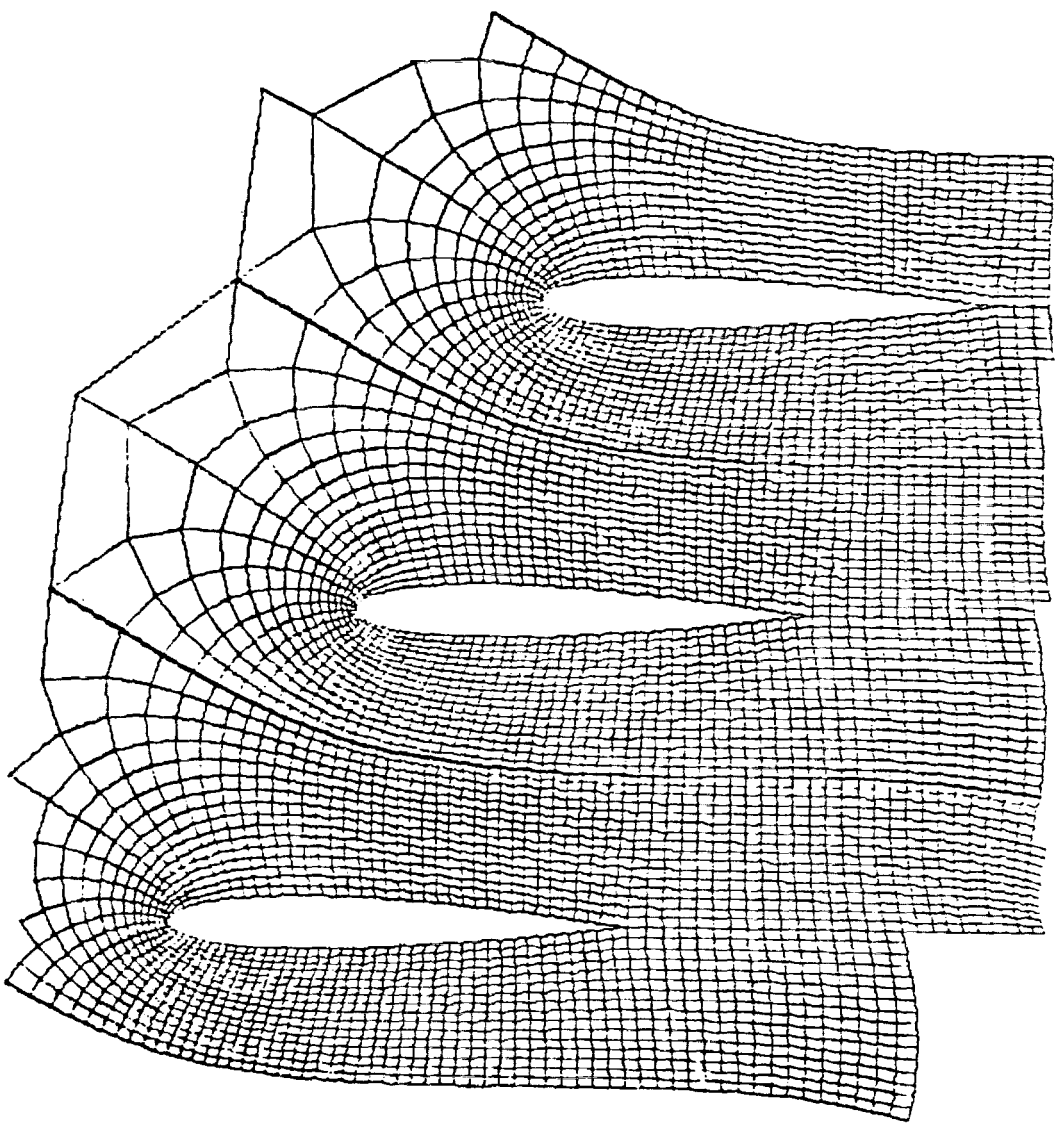

NACA 0012 airfoil. Stagger angle 30.00; pitch 0.794; cascade grid 128 × 16.